Structural changes of B_2O_3 through the liquid-glass transition range: A Raman-scattering study

A. K. Hassan, L. M. Torell, and L. Börjesson
Department of Physics, Chalmers University of Technology, S-412 96 Gothenburg, Sweden

H. Doweidar*
Physics Department, Faculty of Science, Mansoura University, Mansoura, Egypt
(Received 6 January 1992)

Raman scattering of B_2O_3 has been performed from room temperature to 1273 K to study structural changes as the glass transforms into the melt via the supercooled regime. It is found that a structural model containing threefold six-member planar boroxol rings and chains of BO_3 triangles can explain the experimental spectra. From the behavior of the internal vibrations of the boroxol rings and the BO_3 triangles, we conclude that these molecular units do not change significantly as the temperature increases whereas the connectivity of the units is strongly affected. Still, network connectivity is observed in this "strong" liquid far above T_m, where the presence of transverse acoustic modes have also been reported. This supports the idea of a relation between structural properties and the dynamics of the liquid-glass transition as suggested in the "strong-fragile" classification scheme. The structural changes are demonstrated by the intensity profile of the spectra. It is shown that the strongest vibrational mode at 808 cm^{-1}, attributed to the breathing mode of boroxol rings, decreases rapidly in intensity as the temperature is raised above the glass transition temperature T_g. The high-frequency multicomponent band at 1200–1600 cm^{-1} also displays anomalous temperature behavior above T_g. A significant redistribution of the intensity from the two narrow lines at $\sim$1210 and $\sim$1260 cm^{-1} into the broad band at $\sim$1325 cm^{-1} is found. The observed effects are consistent with a gradual breakup of boroxol rings, which change into chains of BO_3 triangles as the temperature increases above T_g. From a detailed analysis of the temperature dependence of the spectra, the structure is estimated to consist of about half of the number of atoms in boroxol rings at T_g. Heating the glass to the melting temperature leads to breaking of about $\frac{1}{3}$ of the boroxol rings.

I. INTRODUCTION

The structural changes that may accompany glass formation in various systems are suggested to be related to their respective dynamics in the supercooled regime.[1,2] In the case of network glasses such as B_2O_3, SiO_2, and GeO_2, with strong covalent interactions, it has been proposed that the transformation to a liquid occur through temperature-activated bond breaking, which may explain the Arrhenius behavior of the viscosity and structural relaxation time in these systems.[2] However, using common techniques for structural studies, such as neutron and x-ray diffraction, and extended x-ray absorption fine structure (EXAFS), only very small changes are observed,[3] which can be accounted for by the change in density. For instance, recent pulsed neutron-diffraction measurements[4] of B_2O_3 reveal the presence of well defined molecular units whose structure does not change significantly with increasing temperature in the wide range from the glassy state to far above the melting temperature, apart from thermally induced fluctuations of bondlengths. Similarly we found that the Brillouin spectra of B_2O_3 are hardly affected by temperature;[5] transverse modes were detected over more than 800 K above T_g, which is the widest range of observation of shear waves so far reported for a glass-forming liquid. Small changes of the structure are often observed more clearly in vibrational spectroscopy and the breaking of bonds in a continuous network is expected to lead to significant changes of the vibrational spectrum, e.g., intensity and softening effects of the involved modes. The aim of the present study is to investigate changes of the vibrational Raman spectrum of B_2O_3 as the temperature is varied from that of the liquid through the supercooled regime to the glassy state and relate these to structural changes.

The structure of vitreous boron oxide (B_2O_3) has been a much debated issue for many years (for a review see Ref. 6). Although it is generally accepted that the molecular building block of vitreous B_2O_3 is the planar BO_3 groups, the manner in which the BO_3 triangles are connected is much discussed. Note that for the continuous-random-network model there is no preferential relative orientation between the triangles required except that dictated by geometrical limits. Some experimental observations of B_2O_3, such as the sharp Raman vibrational mode at 808 cm^{-1},[7] and specific features in the nuclear magnetic resonance[8] (NMR) and nuclear quadrupole resonance[9] (NQR) spectra, give strong indications of well defined molecular entities in the structure suggested to be boroxol rings (B_3O_6). Recent molecular vibrational calculations using a model based on a Bethe lattice of boroxol rings are found to reproduce the experimental Raman spectra very well and also enables one to explain isotope shifts of the vibrational modes.[10] The amount of boron

atoms in boroxol rings was estimated in the NQR study[9] to be ~85%. Accurate neutron-diffraction measurements are reported to be consistent with a structural model containing 60% boroxol rings.[6] In contrast, some molecular-dynamics simulation studies[11,12] demonstrate structures that are absent of boroxol rings and still in good agreement with neutron and x-ray determined structure factors. The general view, however, seems to be that vitreous B_2O_3 consists of a large amount of boroxol rings though the estimated concentration of rings varies. Little is known about the ring concentration in the supercooled and liquid state of B_2O_3.

There are only a few reports on the vibrational behavior of B_2O_3 above T_g,[13] whereas the vibrational spectrum of the glassy state has been extensively investigated.[7,10,13–17] The Raman spectrum of B_2O_3 is markedly different from those of other network glasses. The most prominent feature is the highly polarized, extraordinary sharp (~ 15 cm^{-1}) and very intense mode at 808 cm^{-1}, which from isotope-substitution measurements[15] has been unambiguously attributed to a breathing-type vibration of the plane boroxol ring. Such an assignment is further supported by the sharpness of the peak, which is different from the broad features usually characterizing the disordered network of glass and, which suggests a strongly localized mode.[7,10,13–17]

Other indications of localized dynamics are the two unusually sharp lines of much weaker intensity reported[7,15] at 1210 and 1260 cm^{-1}. In the study of boron and oxygen isotopically substituted glasses[15] they are assigned to B-O stretching vibrations involving both ring and network contributions. The remaining Raman lines are much broader and similar to those of network glasses in general. They have been assigned to various vibrations of the random B-O network.[7,10,17]

In the present study we analyze the boroxol breathing mode at 808 cm^{-1} and the high-frequency band around 1200–1600 cm^{-1}, which is a multicomponent band related to both the boroxol rings and the network. The Raman spectrum of the latter band shows a dramatic redistribution of intensity from boroxol related modes to B-O network related modes as temperature increases. Of special interest is the temperature region around the glass transition for which the structural changes are expected to be initiated and for which there are so far no Raman measurements reported. This range could be investigated by use of a small size sample cell, which would allow that T_g can be passed without breaking the cell.

II. EXPERIMENTAL PROCEDURE

The B_2O_3 glass was prepared from 99.999%-purity B_2O_3 powder, which was vacuum heated at 180 °C for 24 h to reduce any water content. The dehydrated powder was melted in an alumina crucible and a clear bubble free melt was obtained after 4 h at 1000 °C. It was kept for another 24 h at 1000 °C to remove residual water and then quickly cooled into a room-temperature glass. The hygroscopic sample was then transferred to a N_2 atmosphere container where it was broken into smaller pieces and loaded into the optical sample cell. In the remelting process of the glass, when situated in the Raman furnace, bubbles formed and they were removed by heating at 1000 °C in vacuum for about 1 h prior to the Raman measurements. The B_2O_3 sample was contained in a narrow cylindrical quartz tubing (inside diameter 3 mm) with an optical flat window fused to the bottom of the tube. The measurements at high temperatures were performed by means of a cylindrical furnace with three windows, 90° apart, which allowed passage of the laser beam and the detection of 90° scattering. The temperature of the furnace was controlled by an Eurotherm power supply. The temperature of the sample was determined by a chromel-alumel thermocouple placed close to the sample wall. The accuracy of the temperature is ±1 K and the stability better than ±0.5 K over a Raman recording.

The light source is an Ar^+-ion laser (Spectra Physics model 2020) operating at 488 nm with a typical output of 700 mW. The polarization of the incident beam was controlled by a half-wave plate and the scattered light was analyzed by rotating a polarizing prism. Raman spectra were recorded in both *VV* geometry (incident and scattered light is polarized vertical to the scattering plane) and *VH* geometry (perpendicular polarizations). A double monochromator (Spex 1403) with 1800 lines/mm holographic gratings was used to resolve the Raman spectra. The slits were set to give a measureed resolution of 2 cm^{-1}. The scattered light was detected by a cooled photomultiplier (RCA model 31034-76). A Spex DM3000R was used for automatic scanning of the selected frequency range, for photon counting, and for storage of the spectra. Every spectrum obtained is the result of the repeated scanning and accumulation of, on average, 10 spectra. The spectra were corrected for background and thereafter temperature reduced. The reduced spectra $I_R(\omega)$ were obtained from the experimental spectra $I(\omega)$ according to

$$I_R(\omega)=I(\omega)\frac{\omega}{[1+n(\omega,T)]}\ , \tag{1}$$

where $n(\omega,T)$ is the Bose-Einstein population factor. Such a reduction is necessary to be able to compare spectra at different temperatures. A multicomponent fit of a set of lorenzians were applied to each of the observed spectra as discussed below.

III. RESULTS

The Raman spectrum of vitreous B_2O_3 in the 100–1800-cm^{-1} region is shown in Fig. 1(a) for *VV* and *VH* polarization, respectively. Values for the degree of polarization I_{VV}/I_{VH}, frequency $\Delta\nu$, and full width at half height (FWHH) of the strongest mode are shown in the figure. The spectral characteristics are in close agreement with those reported for B_2O_3 in the literature.[7,13–17] The temperature evolution of the spectrum was investigated over a wide range from room temperature through the glass transition temperature [$T_g \approx 533$ K (Ref. 18)] and up to 1273 K. Representative spectra are demonstrated in Fig. 1(b).

Without further analysis some general tendencies are immediately obvious from Fig. 1(b). As temperature in-

creases there is an intensity increase in the low-frequency spectrum around 525 cm^{-1}, in contrast the mode at $\sim$808 cm^{-1} decreases rapidly in strength [see inset in Fig. 1(b)] as is also the case for the higher-frequency range 1200–1300 cm^{-1}, whereas there is an intensity enhancement above 1300 cm^{-1}. In the following we will discuss in detail the behavior of the well defined mode at

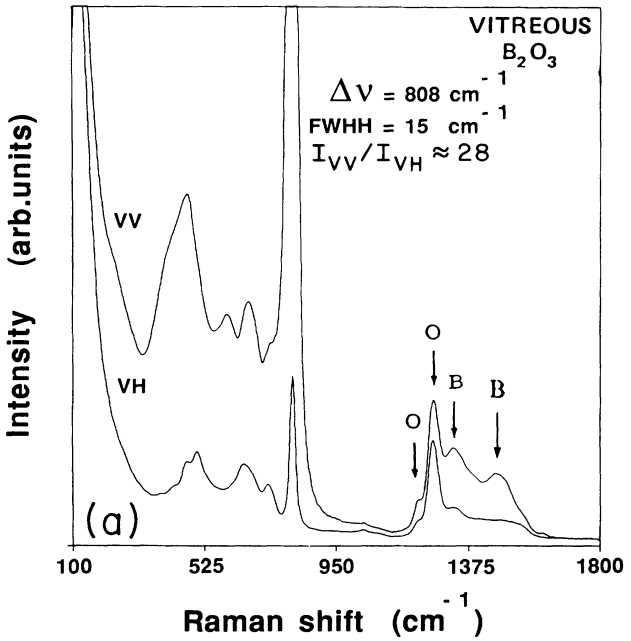

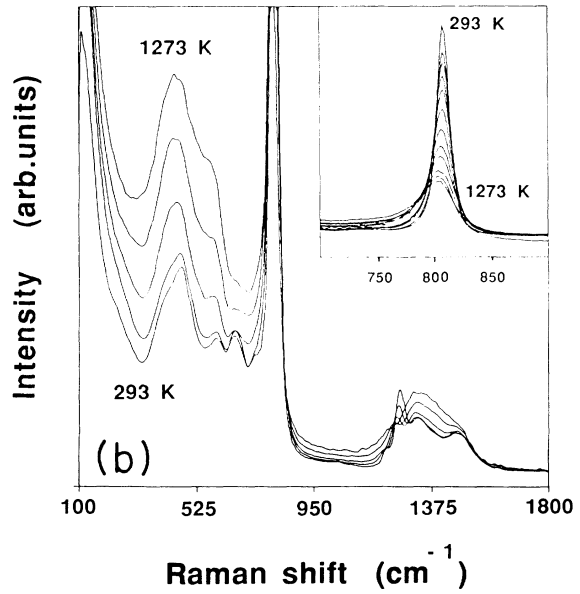

FIG. 1. (a) Room-temperature Raman spectrum of B_2O_3 for *VV* and *VH* polarization. The peak frequency, full width at half height, and polarization ratio of the strongest mode at the 808-cm^{-1} mode are noted. (b) Raman spectra of vitreous and molten B_2O_3 at 293, 373, 533 (T_g), 723 (T_m), and 1273 K. Inset shows Raman spectra of the 808-cm^{-1} mode for different temperatures (293, 473, 533, 573, 673, 723, 773, 873, 973, 1073, 1173, and 1273 K).

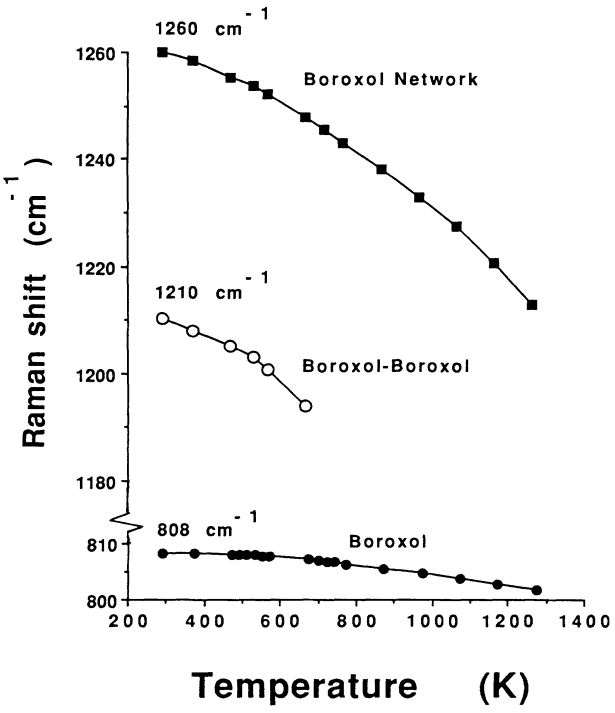

FIG. 2. Temperature dependence of the frequency shift of the 808, 1210, and 1260-cm^{-1} modes. Lines are guides for the eye.

$\sim$808 cm^{-1} and the multicomponent band in the 1200–1600-cm^{-1} range.

The position of the 808-cm^{-1} peak is only weakly temperature dependent, see Figs. 2 and 3, whereas the half width and intensity are strongly affected as demonstrated in Figs. 3 and 4. The results obtained for the room-temperature glass and those from the melt are in good

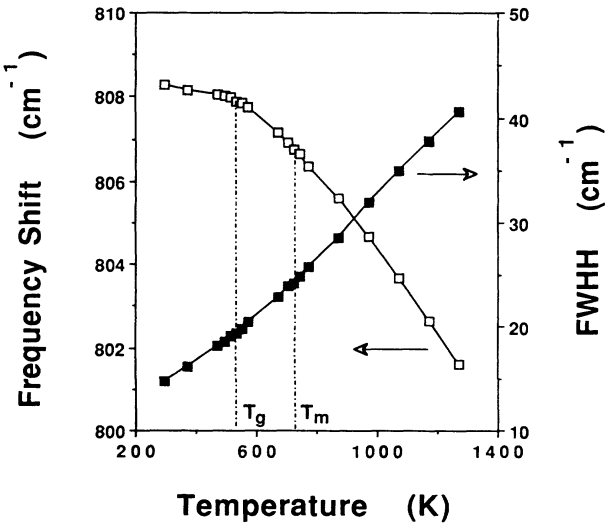

FIG. 3. Temperature dependence of the frequency and half width (full width at half height) of the 808-cm^{-1} mode.

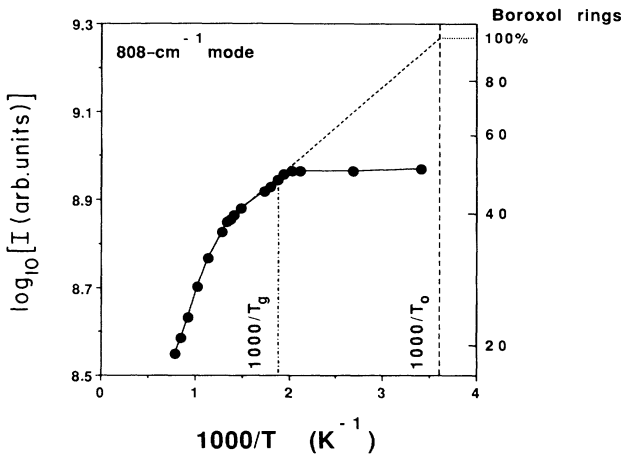

FIG. 4. Inverse temperature dependence of logarithmic integrated intensity of the 808-cm^{-1} mode for vitreous and molten B_2O_3. Right scale indicate the amount of boroxol rings estimated as described in the text.

agreement with previously reported observations.[7,13] There are no literature data available for comparisons for the range from room temperature through the glass transition up to the melting temperature 723 K. It can be seen in Figs. 3 and 4 that this range marks a crossover for all spectral characteristics, especially notable in the case of the frequency and logarithmic intensity, which change from almost constant behavior for $T < T_g$ to strongly temperature dependent above T_g.

The band in the 1200–1600-cm^{-1} region is presented in Fig. 5 for various temperatures. A multicomponent analysis reveal room-temperature components at about

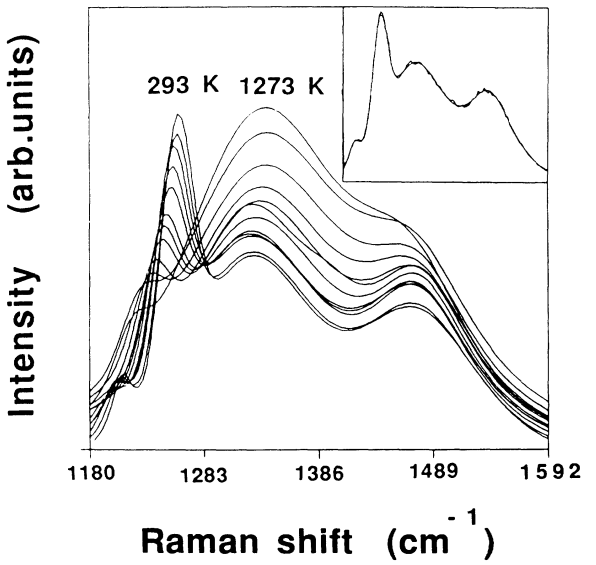

FIG. 5. Raman spectra of the high-frequency multicomponent band of vitreous and molten B_2O_3 at 293, 473, 533, 573, 673, 723, 773, 873, 973, 1073, 1173, and 1273 K. Inset shows experimental curve and curve fit of the multicomponent band at room temperature.

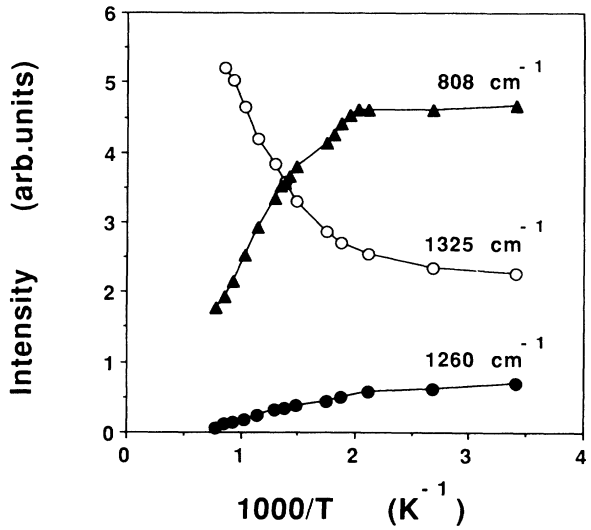

FIG. 6. Integrated Raman intensity of the 808-, 1260-, and 1325-cm^{-1} modes vs temperatures. The intensity of the 808-cm^{-1} mode has been divided by a factor of 2 relative to the intensities of the other modes for clarity.

1210, 1260, 1325, and 1475 cm^{-1}, respectively, in accordance with literature data.[7,15] For the temperature dependencies of the four components, for which there are so far no data reported, we note drastic differences. The lowest-frequency 1210-cm^{-1} mode, which appears as a shoulder on the band, decreases in intensity as temperature increases and was not detectable above T_m. The half width of the component stayed remarkably constant with FWHH$\approx$28 cm^{-1} over this range, whereas the frequency decreased from $\sim$1210 cm^{-1} at room temperature to $\sim$1195 cm^{-1} at 673 K, see Fig. 2. Similar behavior was demonstrated for the 1260-cm^{-1} (room-temperature) mode; a frequency decrease to $\sim$1213 cm^{-1} at 1273 K (see Fig. 2); a constant half width of $\sim$40 cm^{-1}; a dramatic intensity decrease. Data for the intensity of this mode, which was considerably stronger than the 1210-cm^{-1} component and persisted over a wider temperature range, are displayed in Fig. 6. Opposite to the behavior of the 1210 and 1260-cm^{-1} modes, the component at 1325 cm^{-1} increases in strength as temperature increases; see Figs. 5 and 6. Moreover, the half width of the 1325-cm^{-1} component is considerably broader and temperature dependent; a width of $\sim$145 cm^{-1} was observed in the glass, and it increases monotonically with temperature to $\sim$180 cm^{-1} at 1173 K. In contrast, the highest frequency component, identified at 1475 cm^{-1}, is found to be in all respects unaffected by temperature; the intensity, frequency, and half-width (FWHH$\sim$160 cm^{-1}) being, within the accuracy of measurements, constant over the whole temperature range of study.

IV. DISCUSSION

From the analysis of the 800–1800-cm^{-1} range we find that three modes (at 808, 1210, and 1260 cm^{-1}, respectively) decrease in strength, one (at 1325 cm^{-1}) is increasing and one (at 1475 cm^{-1}) is constant as the temperature

is raised. We will first discuss the modes of decreasing intensity and note that for vitreous B_2O_3 they have previously been identified as being related to various oxygen motions.[15,17]

A. The 808-cm^{-1} mode

The strong, sharp, and well polarized peak at $\sim$808 cm^{-1} has been assigned to localized breathing motions of oxygen atoms inside the boroxol ring.[7,10,13–17] Calculations of the vibrational spectrum of an isolated boroxol molecule with the outer oxygen atoms bonded to atoms of variable mass show that the 808-cm^{-1} mode is relatively unaffected by changes of the mass.[7] Later calculations on an infinite network of boroxol units bridged by oxygen atoms demonstrate the evolution of localized modes into delocalized modes.[17] It is then again demonstrated that the 808-cm^{-1} mode remains localized and sharp without any significant broadening on network formation. Recent models based on a Bethe lattice of boroxol rings reproduce the position, intensity and half width of the 808-cm^{1} mode by decoupling the symmetric ring mode from the rest of the lattice.[10]

The assignment of the 808-cm^{-1} line to a decoupled boroxol-ring breathing vibration is supported by the small changes of the vibrational frequency with temperature, see Fig. 2. Raising the temperature 800 K above the glass transition only implies a frequency decrease of less than 7 cm^{-1}. This implies the presence of well defined and (dynamically) isolated molecular species in B_2O_3 even at temperatures high above $T_m = 723$ K, i.e., even in its thermodynamically stable liquid state. Note, however, in Fig. 3 that there is a change at T_g in the temperature dependence of the vibrational frequency. This is in contrast to the findings of a recent neutron-diffraction study,[4] which shows no detectable anomalies in the static and dynamical properties of the B—O bonds through the glass transition. The temperature behavior we observe, though considerably weaker, is similar to that of the specific volume; see Fig. 7.[18,19] Thus we conclude that, while the vibrational data of the 808-cm^{-1} component indeed reflect a highly localized molecular mode, it is not completely decoupled in behavior from the network but is affected by the specific volume changes that occur in the glass transition range.

The intensity profile of the 808-cm^{-1} mode can be taken as a measure of the boroxol-ring concentration. The results in Fig. 4 imply that the concentration is constant from room temperature all the way to the glass transition. Then, at T_g, openings of the boroxol rings are initiated, and above T_g the number of rings rapidly decreases. The data above T_m are in accordance with previous Raman observations of the melt.[13] A calculation of the boroxol-ring concentration based on the intensity of the 808-cm^{-1} mode is discussed in a separate paragraph below.

B. The 1210- and 1260-cm^{-1} modes

Next we focus on the higher-frequency modes at 1210 and 1260 cm^{-1} and note that such narrow lines (28 and 40 cm^{-1}, respectively) are hardly typical for a disordered glassy network in general. From the similar findings of the 808-cm^{-1} mode, it is likely that the 1210- and 1260-cm^{-1} vibrations are related to the well-defined molecular structure of the boroxol ring. Previous Raman data[15] and calculations[17] suggest that these modes are not solely associated with the boroxol ring but represent vibrations involving both ring and network contributions. The situation is schematically represented in Fig. 8, where 8(a) shows a single oxygen atom connecting two rings and in 8(b) the rings are connected via a planar BO_3 triangle. One might also consider bridging via a pair and/or higher orders of BO_3 triangles. However, since it has been shown that the vibrational frequency of the bridging oxygen is rather insensitive to the attached mass,[7] we can take 8(b) as a representative of all those cases. We then attribute the lower-frequency component (1210 cm^{-1}) to

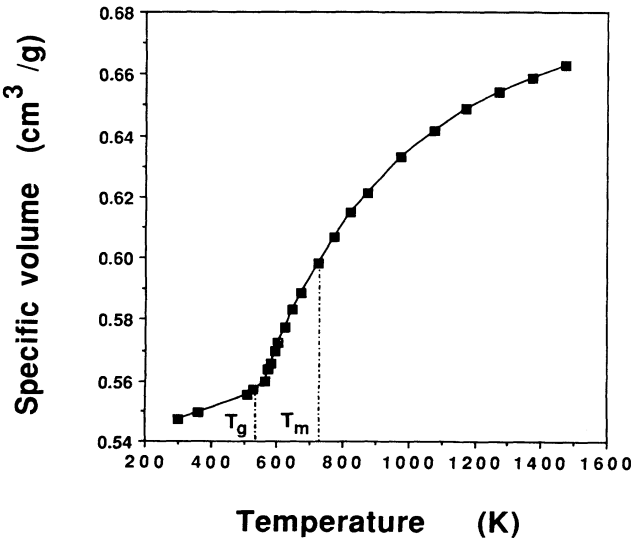

FIG. 7. Specific volume vs temperature. Data taken from Refs. 18 and 19.

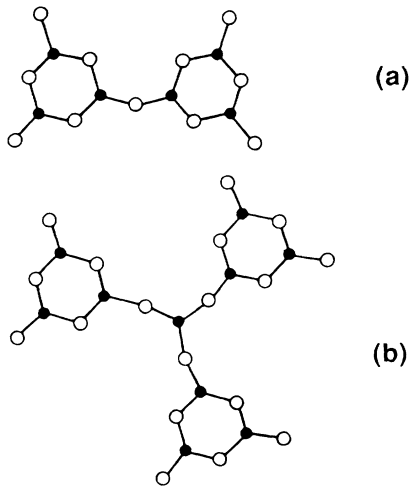

FIG. 8. Schematic pictures of (a) a single oxygen bridging two boroxol rings, and (b) three boroxol rings bridged by a planar BO_3 triangle.

vibrations involved in the bridging via a single oxygen [Fig. 8(a)] and the higher-frequency component (1260 cm^{-1}) to the vibrational motions involving one (or several) planar BO_3 triangle(s) [Fig. 8(b)] as discussed in the following.

Vibrational spectra of isotope substituted B_2O_3 (^{10}B, ^{11}B, ^{16}O, ^{18}O) show that the 1210-cm^{-1} mode is indeed more sensitive to oxygen substitution than the 1260-cm^{-1} mode, both being similarly affected by changes of the boron mass.[15] Next we turn to recent pulsed neutron-diffraction data.[4] The neutron results reveal anomalous damping behavior of the second peak in the radial distribution function as the temperature is raised above T_g. It is interpreted as being due to structural changes caused by changes in the connectivity of BO_3 units as the boroxol units open. It is suggested that the opening of the rings results in a gradual increase of chainlike segments embedded in the three-dimensional network. Comparing with our data for the temperature dependence of the frequency shift of the 1210- and 1260-cm^{-1} modes we also observe anomalous behavior, see Fig. 2. The frequency of both components drop considerably more rapid with temperature than the 808-cm^{-1} mode. For the higher-frequency 1260-cm^{-1} component, which can be followed over a wider temperature range, we notice a frequency drop of ~ 50 cm^{-1} as the temperature is raised some 800 K above the glass transition. In contrast, the frequency of the 808-cm^{-1} mode changes only 7 cm^{-1} over the same temperature range. The findings indicate vibrational softening of the 1210- and 1260-cm^{-1} modes caused by structural changes in the melt. This is in agreement with the neutron observations of changes in the connectivity of the BO_3 units. Thus, the anomalous vibrational softening and the neutron results support the present assignments of the 1210- and 1260-cm^{-1} modes. Finally we turn to the intensity and note that the intensity drop of the 1210- and 1260-cm^{-1} modes follow the behavior of the 808-cm^{-1} mode, see Figs. 1(b) and 6. This is a further support of the assignments of these modes as being related to the bridging of the boroxol rings.

In conclusion we note that, while the intensity behavior of the 808-, 1210-, and 1260-cm^{-1} components demonstrates that they all depend on the concentration of boroxol rings, their dynamics show distinctly different types of behavior. Strongly localized dynamics is observed in the case of the 808-cm^{-1} mode, which is attributed to decoupled vibrations of the boroxol units. Though the amount of rings is rapidly decreasing with increasing temperature, the dynamics show that their molecular structure is little affected by temperature. The connectivity of the network decreases with increasing temperature as the boroxol rings gradually open. The connectivity of the network can be characterized by the viscosity as recently demonstrated in the "strong-fragile" classification scheme presented for a wide range of glass-forming liquids.[2] In this representation, glass-forming B_2O_3 is regarded as a relatively strong liquid. For oxide glasses in general, strong covalent bondings prevent the structure from any drastic changes when temperature is raised above T_g as demonstrated for instance by the relatively small heat capacity changes. Above T_g the high degree of connectivity results in viscosities that only slowly change with temperature and then in an almost Arrhenius manner. This is in contrast with, for instance, glass-forming Coulomb liquids, which generally fall on the other extreme among the fragile liquids in this classification and are represented by Vogel-Tamman-Fulcher viscosity behavior.[2] We have previously investigated the temperature dependence of the elastic properties by Brillouin scattering.[5] The spectra revealed transverse-acoustic modes over an extremely broad temperature range and still detectable at 1200 K, the highest temperatures studied. This implies that the liquid can sustain shear forces even at temperatures high above the melting temperature at 723 K. In the present study, the connectivity of the network is represented by the 1210- and 1260-cm^{-1} modes. We note in Figs. 5 and 6 that the stronger of the two, the 1260-cm^{-1} mode, is indeed clearly visible up to 1200 K. Thus, while a softening of the structure is demonstrated by the large temperature dependence of vibrations of the 1210- and 1260-cm^{-1} mode, their intensity behavior indicates that there is some connectivity of the network even in the high-temperature liquid. This is in accordance with the interpretation of B_2O_3 as a strong liquid and supports the relevance of the strong-fragile classification scheme.[2]

C. The 1325- and 1475- cm^{-1} modes

We now turn to the two highest-frequency components investigated, at 1325 cm^{-1} and 1475 cm^{-1}, respectively. Raman isotope shift data[15] reveal that the modes involve more boron than oxygen motion. The broad half width of the modes (145 and 160 cm^{-1}, respectively) suggests that they are related to the disordered network of BO_3 triangles rather than to the well-defined boroxol rings. This is certainly the case for the 1475 cm^{-1}, which stays more or less unaffected (constant intensity, half width, position) by the opening of the boroxol rings as temperature increases. In contrast, the 1325 cm^{-1} increases rapidly in intensity as the temperature increases, see Fig. 6. The temperature dependence seems to be the reverse to that of the 808-cm^{-1} mode, which is also included in Fig. 6 for comparison. Neutron-diffraction investigations[4] indicate that the opening of the rings is accompanied by that the structure gradually changes into chainlike segments. The behavior of the 1325 cm^{-1} can then be attributed to the unaffected network. Such an assignment implies that the intensity of the 1325-cm^{-1} mode is inversely related to the concentration of boroxol groups as indeed is demonstrated in Fig. 6.

D. The concentration of boroxol rings

Values for the fraction of B atoms in boroxol rings in the vitreous state has been reported over a wide range from nonexisting[11,12] up to such large concentrations as 0.85.[9] In the following, the concentration of rings will be estimated from the temperature dependence of the spectra, starting with the behavior of the 808-cm^{-1} mode.

While the intensity of the 808-cm^{-1} mode shows an in-

creasing concentration of rings in the melt as the temperature is lowered, we note that the crystalline structure of B_2O_3 is proposed to consist of ribbons of interconnected BO_3 triangles and there is no evidence of rings.[20] However, pure B_2O_3 will not crystallize from the melt at atmospheric pressure and this has indeed been explained by assuming a large amount of boroxol units in the melt.[6] The presence of such rings implies a crystallization process that requires considerable rearrangement of the structure and therefore is likely to be by-passed. If, on the other hand, we hypothetically assume that crystallization can be initiated from a melt containing boroxol rings, then the upper limit of the ring concentration in the glass can be estimated as follows. First we note that a periodic structure containing boroxol rings can clearly be designed and any crystalline polymorph would either contain only boroxol groups or else an ordered mixture of boroxol units and independent BO_3 triangles as discussed by Johnson, Wright, and Sinclair.[6] Assuming the crystalline structure to be a network of boroxol species solely, then from the temperature behavior of the intensity of the 808-cm^{-1} mode we estimate the upper limit for the concentration of such species in the liquid near T_g, and hence in the glassy state. Using the integrated intensity I_{808} as a molecular structural indicator of the glass transition, we can extrapolate its behavior in the supercooled regime to $T \rightarrow T_0$ where T_0 is the ideal liquid-glass transition temperature. T_0 can be regarded as the so-called Kauzmann temperature[21] at which the extrapolated entropy of the supercooled liquid equals that for the crystal. It can be estimated by fitting the Vogel-Fulcher relation of the structural relaxation time

$$\tau = \tau_0 \exp[DT_0/(T-T_0)] , \quad (2)$$

using $\tau_0 = 10^{-13.5}$ s, and $D = 35$ as discussed in Ref. 22. This implies an ideal glass transition temperature of 277 K, i.e., considerably lower than that experimentally determined at 533 K. This is in accordance with the assignment of B_2O_3 as a relatively strong glass former in the strong-fragile classification scheme of Angell.[2] The Raman intensity of a crystal containing only boroxol rings can now be estimated by extrapolating the integrated intensity I_{808} to T_0. Since the system gets dynamically arrested at T_g, the behavior at the ideal glass transition must be derived from extrapolating the data obtained above T_g. Then we take the supercooled liquid to be at equilibrium above T_g although it is in a metastable state compared to the crystal. Assuming I_{808} to be linearly correlated to the concentration of boroxol rings and the concentration to be of Arrhenius behavior we extrapolate in Fig. 4 to the suggested fully developed ring structure at T_0 and use it to estimate the intensity ratio at the glass transition, $I_{808}(T_g)/I_{808}(T_0)$, to be $\sim 49\%$. Vibrational spectra of isotopic compositions of B_2O_3 glasses show that the 808-cm^{-1} band is due only to the oxygen motions and no changes are observed for changes of the boron mass.[15] Based on our estimations we then conclude that for the glass the ratio of O atoms in boroxol rings to the total amount of oxygens in the vitreous structure is limited to a maximum fraction of $\sim 50\%$. The experimental accuracy is estimated to $\pm 15\%$ and includes errors in the intensity measurements in τ_0, D, and T_g for the determination of T_0.

Next we estimate the amount of boroxol rings by making use of a model, suggested in the neutron-diffraction study[4] and supported by the present observations, of a structure that contains an increasing amount of chainlike segments as temperature increases due to openings of the boroxol rings. We take the temperature dependence of the 808-cm^{-1} mode as a characteristic of the temperature behavior of the ring concentration. The temperature dependence of the 1325-cm^{-1} mode, which is reverse to that of the 808-cm^{-1} mode, is taken as a signature of the change in the amount of chain segments. The 1425-cm^{-1} mode, which is unaffected by temperature, is taken as representing the unmodified network. The fractions of these units depend on temperature. However, they are assumed to represent the complete structure according to

$$N_{\text{rings}} + N_{\text{chains}} + N_{\text{network}} = 1 . \quad (3)$$

The fraction of boroxol rings N_{rings} is given by I_{808}/A, where I is the intensity and A is the Raman cross section of this mode. The fractions of chains can be represented by I_{1325}/B, where B is the corresponding cross section for the 1325-cm^{-1} mode, and similarly the unmodified network gives a constant contribution represented by the intensity of the 1425-cm^{-1} mode. Fitting the intensity data of the various modes at different temperatures to Eq. (3), using the respective Raman cross sections as fitting parameters, we obtain the results presented in Fig. 9. It can be seen that the dramatic temperature dependence of the 808-cm^{-1} mode is consistent with the reverse dependence of the 1325-cm^{-1} mode for a structure containing $\sim 60\%$ boroxol rings in the glass and $\sim 45\%$ at the melting temperature.

Finally we will estimate the boroxol content from vibrational density-of-states considerations. It has been shown that for oxide glasses the depolarized Raman spectrum roughly displays the density of states[23] and therefore the depolarized spectrum can be used directly in the

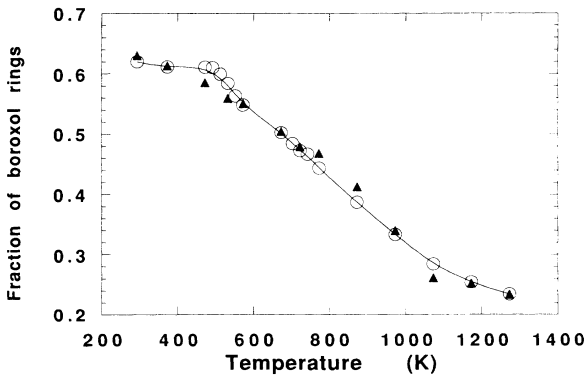

FIG. 9. Temperature dependence of the fraction of boroxol rings of the structure as calculated from the model represented by Eq. (3). Open rings and filled triangles represent values obtained from the temperature dependencies of the 808- and 1325-cm^{-1}, modes, respectively.

analysis. We estimate the concentration of boroxol rings by comparing the depolarized intensity of the breathing mode of the ring, I_{808} (depol), to the depolarized modes representing the network; see Fig. 1(a). We therefore calculate the integrated intensity of the high-frequency band at 1200–1600 cm^{-1} at the highest temperature of observation, i.e., when the concentration of rings is small and hardly affects the band profile. Then the band can be taken as representing the vibrational dynamics from all atoms of the "opened" structure. In the comparison we use twice the integrated intensity of I_{808}, since isotope substitution shows that only the oxygens take part in the symmetric 808-cm^{-1} vibration, the borons being at rest. From the ratio of twice the intensity of the I_{808} (depol) mode to the intensity of the band $I_{1200-1600}$ (depol) a value of ~60% boroxol groups is estimated to be present in the glass. This is in good correspondence with the values (50 and 60%) obtained from the temperature dependencies of I_{808} and I_{1325} modes. In a simple density-of-states calculation based on a model with ~75% of the boron atoms in boroxol rings, qualitative agreement is obtained with inelastic neutron-scattering results.[24]

V. CONCLUSION

By the use of a thin sample, Raman spectroscopy could be carried out on B_2O_3 from room temperature through the glass transition up to temperatures of ~1300 K. Several striking anomalies in the dynamics are observed. The 808-, 1210-, and 1260-cm^{-1} modes, which previously have been assigned to involve mainly oxygen vibrations, show both similarities and differences. For the 808-cm^{-1} component we find only small frequency changes, even though the temperature is raised high above the melting temperature. The mode displays the typical localized dynamics characteristic of well defined species as has already been reported from numerous spectroscopic and calculation studies. Accordingly, the 808-cm^{-1} component has been assigned to the breathing vibration of boroxol rings. In contrast the 1210 and 1260-cm^{-1} modes reveal softening as the temperature is raised above the glass transition temperature, which suggests that the system is exposed to considerable structural changes. We assign the 1210- and 1260-cm^{-1} modes to the vibration of oxygens bridging two boroxol rings, respectively, bridging a boroxol ring to the network of BO_3 units. The intensities of the 808-, 1210-, and 1260-cm^{-1} components all decreases as temperature increases. This together with the softening of the higher-frequency modes, suggest a decreasing concentration of boroxol rings followed by substantial rearrangements of the structure as temperature increases above T_g. The opening of the boroxol rings is initiated at the glass transition whereas below T_g the concentration stays constant. The structural rearrangements follow similar temperature dependence as that of the specific volume.

The highest-frequency modes analyzed, i.e., at 1325 and 1475 cm^{-1}, respectively, have previously been assigned to mainly the dynamics of B in the network. From the rapid intensity increase of the 1325-cm^{-1} mode as the temperature is raised, which is the reverse of the behavior of the 808-cm^{-1} component, we assign this mode to B-O vibrations of BO_3 units released as the boroxol opens. The 1475-cm^{-1} mode stays in all respects unaffected by temperature. The findings support recent suggestions based on neutron-scattering data that the BO_3 units do not change significantly with temperature whereas the connectivity of these units changes. It is proposed that as temperature increases and the boroxol units open the structure becomes more and more chainlike. Then the 1325-cm^{-1} component may be attributed to the chainlike segments that gradually increase in concentration as the structure of boroxol rings breaks down, whereas the 1475-cm^{-1} mode may represent the unaffected network of BO_3 units.

The concentration of boroxol ring was estimated from independent observations of (1) the temperature dependence of the boroxol vibration assuming a perfect crystalline structure of only boroxol rings at the ideal glass transition temperature, (2) the temperature dependence of the concentration of segments of BO_3 units created as the boroxol units open, and (3) density-of-state considerations. All the data are consistent with a structure for vitreous B_2O_3, which contains about half of the number of atoms in boroxol rings.

ACKNOWLEDGMENTS

This work has been supported by the Swedish Natural Science Foundation. One of us (A. K. Hassan) gratefully acknowledges financial support from the Ministry of Higher Education, Mission Department, Egypt.

*Present address: Physics Department, Faculty of Sana'a, Sana'a University, Sana'a P.O.B. 13410, Republic of Yemen.

[1]S. Brawer, *Relaxation in Viscous Liquids and Classes* (American Ceramic Society, Columbus, OH, 1985).
[2]C. A. Angell, J. Phys. Chem. Solids **49**, 863 (1988).
[3]S. R. Elliott, *Physics of Amorphous Solids* (Longman, New York, 1984).
[4]M. Misawa, J. Non-Cryst. Solids **122**, 33 (1990).
[5]M. Grimsditch, R. Bhadra, and L. M. Torell, Phys. Rev. Lett. **62**, 2616 (1989).
[6]P. A. V. Johnson, A. C. Wright, and R. N. Sinclair, J. Non-Cryst. Solids **50**, 281 (1982).
[7]F. L. Galeener, G. Lucovsky, and J. C. Mikkelsen, Jr., Phys. Rev. B **22**, 3983 (1980).
[8]G. E. Jellison, Jr., L. W. Panek, P. J. Bray, and G. B. Rouse, Jr., J. Chem. Phys. **66**, 802 (1977).
[9]S. J. Gravina, P. J. Bray, and G. L. Petersen, J. Non-Cryst. Solids **123**, 165 (1990); P. J. Bray, J. F. Emerson, D. Lee, S. A. Feller, D. L. Bain, and D. A. Feil, *ibid.* **129**, 240 (1991).
[10]R. A. Barrio, F. L. Castillo-Alvadore, and F. L. Galeener, Phys. Rev. B **44**, 7313 (1991).
[11]T. F. Soules, J. Chem. Phys. **73**, 4032 (1980).
[12]W. Soppe, C. van der Marel, W. F. van Gunsteren, and H. W. Hartog, J. Non-Cryst. Solids **103**, 201 (1988).
[13]G. E. Walrafen, S. R. Samanta, and P. N. Krishnan, J. Chem. Phys. **72**, 113 (1980).

[14]T. W. Bril, Philips Res. Rep. Suppl. **2**, 1 (1976).
[15]C. F. Windisch, Jr. and W. M. Risen, Jr., J. Non-Cryst. Solids **48**, 307 (1982).
[16]F. L. Galeener and A. E. Geissberger, Phys. Rev. B **27**, 6199 (1983).
[17]F. L. Galeener and M. F. Thorpe, Phys. Rev. B **28**, 5802 (1983).
[18]P. B. Macedo, W. Capps, and T. A. Litovitz, J. Chem. Phys. **44**, 3357 (1966).
[19]A. Napolitano, P. B. Macedo, and E. G. Hawkins, J. Am. Ceram. Soc. **48**, 613 (1965).
[20]S. L. Strong and R. Kaplow, Acta Crystallogr. B **24**, 1032 (1968).
[21]W. Kauzmann, Chem. Rev. **43**, 219 (1948).
[22]M. Grimsditch and L. M. Torell, in *Dynamics of Disordered Materials,* edited by D. Richter, A. J. Dianoux, W. Petry, and J. Texeira (Springer, Berlin, 1989), p. 196.
[23]See, for example, F. L. Galeener, J. Non-Cryst. Solids **123**, 182 (1990).
[24]A. C. Hannon, R. N. Sinclair, J. A. Blackman, A. C. Wright, and F. L. Galeener, J. Non-Cryst. Solids **106**, 116 (1988).